

## Parallel computation of supersonic reactive flows with detailed chemistry

**Scott G. Sheffer**  
*Princeton Univ., NJ*

**Antony Jameson**  
*Princeton Univ., NJ*

**Luigi Martinelli**  
*Princeton Univ., NJ*

**AIAA, Aerospace Sciences Meeting & Exhibit, 35th, Reno, NV, Jan. 6-9, 1997**

This paper presents parallel computations of high speed steady-state hydrogen/oxygen and hydrogen/air reactive flows. The governing equations for reactive flow in the absence of viscosity, thermal conductivity and species diffusion effects are solved using an explicit algorithm while treating the chemical source terms in a point-implicit manner. The convective upwind and split pressure scheme is used to provide necessary artificial dissipation without contaminating the solution. Results indicate excellent parallel speedups along with adequate resolution of the reaction zone in both 1D nozzle and axisymmetric test cases. (Author)

# Parallel Computation of Supersonic Reactive Flows with Detailed Chemistry

Scott G. Sheffer\*, Antony Jameson†, and Luigi Martinelli‡  
 CFD Laboratory for Engineering Analysis and Design  
 Department of Mechanical and Aerospace Engineering  
 Princeton University  
 Princeton, New Jersey 08544 U.S.A.

## Abstract

This paper presents parallel computations of high speed steady-state hydrogen/oxygen and hydrogen/air reactive flows. The governing equations for reactive flow in the absence of viscosity, thermal conductivity and species diffusion effects are solved using an explicit algorithm while treating the chemical source terms in a point implicit manner. The CUSP (Convective Upwind and Split Pressure) scheme is used to provide necessary artificial dissipation without contaminating the solution. Results indicate excellent parallel speedups along with adequate resolution of the reaction zone in both one-dimensional nozzle and axisymmetric test cases.

## Nomenclature

$\mathbf{C}(w_{ij})$	convective Euler fluxes
$\mathbf{D}(w_{ij})$	dissipative fluxes
$d_{j+\frac{1}{2}}$	diffusive flux at cell interface
$E$	total energy (internal, chemical and kinetic)
$\mathbf{f}, \mathbf{g}$	Euler flux vectors
$\mathbf{H}$	source vector Jacobian
$H$	mixture total enthalpy
$h_i$	static enthalpy of species $i$
$M$	Mach number
$p$	static pressure
$R$	mixture gas constant
$\mathcal{R}$	universal gas constant
$\mathbf{R}(w_{ij})$	total flux residual for cell $i, j$
$T$	static temperature
$u, v$	Cartesian velocity components
$V_{ij}$	volume of cell $i, j$
$\mathbf{w}$	vector of flow variables

$\Delta w_{j+\frac{1}{2}}$	central difference of flow variables at cell interface
$\gamma$	mixture ratio of specific heats
$\rho$	density
$\rho_i$	density of species $i$
$\dot{\omega}$	chemical source term
$\Omega, \partial\Omega$	cell element and boundary

## Introduction

The simulation of high speed chemically reacting flows is a very challenging area for computational efforts. The presence of shock waves necessitates good shock capturing properties, while chemical reactions require avoiding excessive numerical dissipation so that the solution remains uncontaminated. Exponential increases and decreases of radical species in small spatial zones lead to large gradients that must simultaneously be captured without oscillation and without unnecessary dissipation. In addition, the stiff nature of the chemical source terms makes the integration of the governing equations very difficult and time consuming.

The inherent inaccuracy of chemical rate data presents another challenge to modelling reactive flows. The turn around time of reactive flow simulations must be made short enough so that varying rate coefficients may be examined to determine which set is the most appropriate for modelling a particular phenomena.

Because most chemical reactions have characteristic times much less than those of the convective flow field, many explicit schemes are handicapped in computing such flows. The time step for an explicit scheme is proportional to the shortest characteristic time, so that stability restrictions require very short time steps in reactive flow simulations. This short time step leads to very long simulation times for steady state computations.

Several ways to overcome this limitation of explicit

Copyright ©1997 by the Authors. Published by the AIAA Inc. with permission

\* Graduate Student, Student Member AIAA

†James S. McDonnell Distinguished University Professor of Aerospace Engineering, AIAA Fellow

‡Assistant Professor of Aerospace Engineering, AIAA Member

schemes have been explored. The first is to use a fully implicit scheme for the steady state computation, thus removing stability limitations completely. Wilson and MacCormack [4] used such a scheme to compute hydrogen-air combustion over high speed blunt projectiles. Shuen and Yoon [7] used an LU-SSOR scheme to compute pre-mixed and non-pre-mixed chemically reacting flow including viscous effects. Ju [19] implemented an LU-SGS scheme to calculate several reactive viscous flows. These implicit methods may accelerate convergence to steady state, but entails inverting large numbers of matrices and link the solution domain together in a way that may hamper parallelization. In addition, for unsteady simulations, the restriction on the time step for time accuracy may be the dominant factor, removing the advantage gained by the unconditional stability of the implicit scheme.

Another way of reducing the effect of the chemical term stiffness is to treat the source term in a point implicit manner. In this formulation due to Bussing and Murman [9], the source term at the next time level is linearized about the current time level, leading to a fully explicit equation at the cost of a matrix inversion. This action has the effect of pre-conditioning the species continuity equations, rescaling the chemical characteristic time so that it is of the same order as the convective characteristic time. Bussing and Murman also approximated the source term Jacobian matrix by using only its diagonal elements. A considerable savings in computing time was achieved, but the approximation introduces some inaccuracies in the time scaling of the species equations. If these inaccuracies are severe enough, the scheme may become unstable. Eklund et al. [12] investigated several variants of the point implicit procedure. Eberhardt and Imlay [20] suggested scaling the linearized time step by a characteristic time for each species equation and Ju [19] offered a means for determining the characteristic time for each species. Numerous investigators have used the point implicit approach for both steady state [8, 18] and unsteady simulations [10, 5].

Another option is to split the reactive portion and the non-reactive portion of the governing equation and use different solvers on each portion [28]. Thus, a stiff equation solver or asymptotic method could be used for the ordinary differential equations that include the chemical source terms and a highly optimized flow solver could be used for the convective and dissipative parts of the governing equation. However, this may not lead to a true balance of terms in the resulting steady state equation and thus may incorrectly model the interaction between convection, diffusion and reaction.

The accurate capture of shock waves and large gra-

dients in species concentrations necessitates non-oscillatory numerical dissipation schemes that do not overly dissipate the solution. Unphysical diffusion of radical species can lead to gross errors in the prediction of reaction zones and induction times. Oscillations in temperature and pressure may lead to inaccurate production and destruction of radicals. The Total Variation Diminishing (TVD) approach has been taken by several investigators [5, 6, 8, 10, 18] to try to accurately capture shock waves and reaction fronts. Yee and Shinn [15] investigated several aspects of semi-implicit and fully implicit shock-capturing methods for reacting flow. Ju [19] used a fourth order MUSCL scheme with Steger-Warming flux vector splitting to calculate reactive flows. Jameson [22, 23] has presented a framework for Local Extremum Diminishing (LED) and Essentially Local Extremum Diminishing (ELED) schemes which have been shown to have excellent shock capturing qualities for non-reactive perfect gas flows. One of these schemes, Convective Upwind and Split Pressure (CUSP), has good shock capturing properties but has not yet been applied to reactive flows.

In this work, the point-implicit formulation of Bussing and Murman is combined with an explicit time-stepping Euler solver [13] using CUSP dissipation to compute high speed reactive flows. Species diffusion, viscous and thermal conduction effects are neglected due to the large convective speed of the flow [4]. The fully explicit algorithm is parallelized using the MPI standard on an IBM SP-2 to achieve high parallel speedups.

### Governing Equations

The two-dimensional Euler equations with chemical reactions can be written in a Cartesian coordinate system  $(x, y)$  as:

$$\frac{\partial \mathbf{w}}{\partial t} + \frac{\partial \mathbf{f}}{\partial x} + \frac{\partial \mathbf{g}}{\partial y} = \dot{\mathbf{w}}, \quad (1)$$

where  $\mathbf{w}$  is the vector of flow variables,  $\mathbf{f}$  and  $\mathbf{g}$  are the convective flux vectors and  $\dot{\mathbf{w}}$  is the vector of source terms. Consider a control volume  $\Omega$  with boundary  $\partial\Omega$ . The equations of motion of the fluid can then be written in integral form as

$$\frac{d}{dt} \iint_{\Omega} \mathbf{w} \, dx \, dy + \oint_{\partial\Omega} (\mathbf{f} \, dy - \mathbf{g} \, dx) = \iint_{\Omega} \dot{\mathbf{w}} \, dx \, dy, \quad (2)$$

where  $\mathbf{w}$  is the vector of flow variables

$$\mathbf{w} = \begin{Bmatrix} \rho_i \\ \rho u \\ \rho v \\ \rho E \end{Bmatrix},$$

$\mathbf{f}$ ,  $\mathbf{g}$  are the Euler flux vectors

$$\mathbf{f} = \begin{Bmatrix} \rho_i u \\ \rho u^2 + p \\ \rho uv \\ \rho E u + p u \end{Bmatrix}, \quad \mathbf{g} = \begin{Bmatrix} \rho_i v \\ \rho v^2 + p \\ \rho v u \\ \rho E v + p v \end{Bmatrix},$$

and  $\dot{\omega}$  is the chemical source vector

$$\dot{\omega} = \begin{Bmatrix} \dot{\omega}_i \\ 0 \\ 0 \\ 0 \end{Bmatrix}.$$

In these equations,  $i = 1, \dots, N$  and  $N$  is the number of species. For a thermally perfect gas, pressure may be determined from

$$p = \rho RT$$

where  $R$  is the mixture gas constant. The density is found from

$$\rho = \sum_{i=1}^N \rho_i.$$

Temperature may be determined from the following relation,

$$E = e + \frac{1}{2}(u^2 + v^2) = \sum_{i=1}^N \frac{\rho_i}{\rho} h_i - \frac{p}{\rho} + \frac{1}{2}(u^2 + v^2)$$

where  $h_i$  are the individual species enthalpies which depend solely on temperature for a thermally perfect gas.

### Chemical Model

Two different chemistry models are used in this paper. The first is a reduced equation model for hydrogen and air combustion due to Evans and Schexnayder [1] involving seven species and eight reactions. Nitrogen in this set is treated as an inert diluent. The second group of rate equations is the nine species, nineteen reaction modified model of Jachimowski [2] and Wilson and MacCormack [4]. Again, nitrogen is treated as an inert diluent because reactions involving nitrogen have been determined to be negligible below Mach 5 [5].

Both models mentioned here have been well validated in their range of application. Specifically, the Evans and Schexnayder model has been shown to be adequate when ignition is known to be fast. With the length scales and speeds of the problems considered here, ignition is fast. However, due to the lack of some radicals and reactions, the Evans and Schexnayder model may not be completely adequate to describe the details of the induction zone and may fail to provide an accurate representation of the chemistry at very high Mach numbers and temperatures.

The Jachimowski mechanism has been well validated by numerous experiments and computations for high speed reactive flows.

The chemical source terms are computed in the Arrhenius form, with the forward rate coefficients,  $k_{fj}$ , given by

$$k_{fj} = A_j T^{n_j} \exp\left(\frac{-E_{A_j}}{RT}\right) \quad (3)$$

where  $E_{A_j}$  is the activation energy of the  $j$ th forward reaction. The reverse rate coefficients are evaluated using the equilibrium constant for concentration

$$K_{c_j} = \frac{k_{fj}}{k_{b_j}}. \quad (4)$$

This concentration equilibrium constant is obtained from the equilibrium constant in terms of partial pressures:

$$K_{c_j} = K_{p_j} \left(\frac{p_{atm}}{RT}\right)^{\sum_{i=1}^N \nu_{ij}} \quad (5)$$

where  $N$  is the number of species and  $\nu_{ij}$  is the change in the number of moles of species  $i$  in reaction  $j$ . The equilibrium constant  $K_{p_j}$  is calculated from the standard Gibbs free energy change for each reaction. Standard state free energy and species enthalpy information is obtained from the NASA polynomial set [3]. Combining the polynomial representation of the enthalpies with the energy equation yields an implicit equation for temperature which is solved by Newton iteration.

### Numerical Model

#### Flow Equations

The Euler equations are solved using a conservative explicit second-order accurate finite volume formulation in which the chemical source terms are treated point implicitly.

When the integral governing equations (2) are independently applied to each cell  $i, j$  in the domain, we obtain a set of coupled ordinary differential equations of the form

$$\frac{d}{dt}(\mathbf{w}_{ij})V_{ij} + \mathbf{C}(\mathbf{w}_{ij}) + \mathbf{D}(\mathbf{w}_{ij}) = \dot{\omega}V_{ij}, \quad (6)$$

where  $\mathbf{C}(\mathbf{w}_{ij})$  are the convective Euler fluxes,  $\mathbf{D}(\mathbf{w}_{ij})$  are the artificial dissipation fluxes added for numerical stability reasons and  $\dot{\omega}V_{ij}$  are the chemical source terms. This equation (6) can be rewritten as follows (drop the  $i, j$  subscripts for clarity):

$$\frac{d}{dt}[\mathbf{w}]V + \mathbf{R}(\mathbf{w}) = \dot{\omega}V, \quad (7)$$

where  $\mathbf{R}$  is the sum of the two flux contributions. The governing ordinary differential equations are solved using a standard five-stage time stepping scheme [26].

### Chemical Source Terms

The chemical source vector  $\dot{\omega}$  was treated in a point implicit manner [9]. An explicit treatment of the source terms leads, in general, to a time step restriction due to the stability limitation of the explicit scheme. This time step can be orders of magnitude less than the time step of the convective terms. Treating the source terms implicitly removes the stability criterion at the expense of a matrix inversion. The point implicit treatment has the result of reducing the stiffness of the problem by effectively rescaling the characteristic time of the reactions so that their magnitudes are commensurate with the convective characteristic time. We begin by writing the governing ordinary differential equation for cell  $i, j$  but instead evaluate the chemical source vector at the next time level:

$$\frac{d}{dt}[\mathbf{w}]V + \mathbf{R}(\mathbf{w}^n) = \dot{\omega}^{n+1}V. \quad (8)$$

We then linearize the chemical source vector about the present time level so that

$$\dot{\omega}^{n+1} \approx \dot{\omega}^n + \frac{\partial \dot{\omega}^n}{\partial \mathbf{w}} \frac{d}{dt}[\mathbf{w}]\Delta t. \quad (9)$$

Substituting this into the governing equation gives the following expression

$$\frac{d}{dt}[\mathbf{w}]V + \mathbf{R}(\mathbf{w}^n) = \dot{\omega}^n V + \frac{\partial \dot{\omega}^n}{\partial \mathbf{w}} \frac{d}{dt}[\mathbf{w}]\Delta t V \quad (10)$$

which, when rearranged, leads to

$$\left[ \mathbf{I} - \Delta t \frac{\partial \dot{\omega}^n}{\partial \mathbf{w}} \right] \frac{d}{dt}[\mathbf{w}]V + \mathbf{R}(\mathbf{w}^n) = \dot{\omega}^n V. \quad (11)$$

This equation is evaluated entirely at the current time level and is thus fully explicit. Finally, the preceding equation may be written as

$$\frac{d}{dt}[\mathbf{w}]V = \left[ \mathbf{I} - \Delta t \frac{\partial \dot{\omega}^n}{\partial \mathbf{w}} \right]^{-1} [\dot{\omega}^n V - \mathbf{R}(\mathbf{w}^n)] \quad (12)$$

This treatment necessitates the inversion of the source term Jacobian matrix

$$\mathbf{I} - \Delta t \mathbf{H} = \mathbf{I} - \Delta t \frac{\partial \dot{\omega}}{\partial \mathbf{w}}$$

with dimension  $N \times N$  where  $N$  is the number of species present in the flow. An inversion for the momentum and energy equations is not necessary due to the absence of chemical source terms in those equations. This  $N \times N$  inversion is done only during the first stage of each time step of the solver and is retained and used for the succeeding four stages. This time-saving measure has no effect on the results of the computation.

Because the chemical source terms have been treated implicitly, the time step limitation of the explicit time integration scheme depends solely on the spectral radius of the flux Jacobian.

### Numerical Dissipation

The Convective Upwind and Split Pressure (CUSP) scheme provides excellent resolution of shocks at high Mach numbers at a reasonable computational cost [22, 23]. For simplicity, let us work in one dimension; extension to higher dimensions is straightforward. We consider the convective and pressure fluxes

$$f_c = u \begin{Bmatrix} \rho_i \\ \rho u \\ \rho H \end{Bmatrix} = u w_c, \quad f_p = \begin{Bmatrix} 0 \\ p \\ 0 \end{Bmatrix}$$

separately. Upwinding of the convective flux is achieved by

$$d_{c_{j+\frac{1}{2}}} = \left| u_{j+\frac{1}{2}} \right| \Delta w_{c_{j+\frac{1}{2}}} = |M| c_{j+\frac{1}{2}} \Delta w_{c_{j+\frac{1}{2}}},$$

where  $M$  is the local Mach number attributed to the interval. Upwinding of the pressure is achieved by

$$d_{p_{j+\frac{1}{2}}} = \text{sign}(M) \begin{Bmatrix} 0 \\ \Delta p_{j+\frac{1}{2}} \\ 0 \end{Bmatrix}.$$

Full upwinding of both  $f_c$  and  $f_p$  is incompatible with stability in subsonic flow, since pressure waves with the speed  $u - c$  would be traveling backwards, and the discrete scheme would not have a proper zone of dependence. Since the eigenvalues of  $\frac{\partial f_c}{\partial w}$  are  $u$ ,  $u$  and  $\gamma u$ , while those of  $\frac{\partial f_p}{\partial w}$  are 0, 0 and  $-(\gamma - 1)u$ , a split with

$$f^+ = f_c, \quad f^- = f_p$$

leads to a stable scheme, similar to that used by Denton [24], in which downwind differencing is used for the pressure.

This scheme does not reflect the true zone of dependence in supersonic flow. Thus one may seek a scheme with

$$d_{c_{j+\frac{1}{2}}} = f_1(M) c_{j+\frac{1}{2}} \Delta w_{c_{j+\frac{1}{2}}}$$

$$d_{p_{j+\frac{1}{2}}} = f_2(M) \left\{ \begin{array}{c} 0 \\ \Delta p_{j+\frac{1}{2}} \\ 0 \end{array} \right\},$$

where  $f_1(M)$  and  $f_2(M)$  are blending functions with the asymptotic behavior  $f_1(M) \rightarrow |M|$  and  $f_2(M) \rightarrow \text{sign}(M)$  for  $|M| > 1$ . Also the convective diffusion should remain positive when  $M = 0$ , while the pressure diffusion must be antisymmetric with respect to  $M$ . A simple choice is to take  $f_1(M) = |M|$  and  $f_2(M) = \text{sign}(M)$  for  $|M| > 1$ , and to introduce blending polynomials in  $M$  for  $|M| < 1$  which merge smoothly into the supersonic segments. A quartic formula

$$f_1(M) = a_o + a_2 M^2 + a_4 M^4, \quad |M| < 1$$

preserves continuity of  $f_1$  and  $\frac{df_1}{dM}$  at  $|M| = 1$  if

$$a_2 = \frac{3}{2} - 2a_o, \quad a_4 = a_o - \frac{1}{2}.$$

Then  $a_o$  controls the diffusion at  $M = 0$ . For transonic flow calculations a good choice is  $a_o = \frac{1}{4}$ , while for very high speed flows it may be increased to  $\frac{1}{2}$ . A suitable blending formula for the pressure diffusion is

$$f_2(M) = \frac{1}{2} M(3 - M^2), \quad |M| < 1.$$

The CUSP splitting is combined with a LED or ELED limiter to achieve second order accuracy in smooth regions with oscillation-free capture of shocks and large gradient regions.

### Boundary Conditions

For one-dimensional nozzle computations, the inflow boundary is taken to be supersonic while the downstream boundary has an imposed back pressure to create a shock in the diverging section of the nozzle.

In the case of external flow cases, the surface boundary is modelled as an adiabatic, non-catalytic inviscid surface. Due to the supersonic nature of the flow, outflow boundary quantities are extrapolated from the interior and inflow quantities are taken to be free stream values.

Free stream and inlet flow values of radical species are set to a mass fraction of  $1 \times 10^{-12}$ . Varying this value did not affect the results.

### Parallelization

The MPI standard is used to parallelize the code on an IBM SP-2. A static domain decomposition with two-level halos for flow quantities and one-level halos for grid information is used. The current point implicit scheme will achieve a higher level of speedup

as compared to a convective flow code alone due to the greater number of operations that take place per cell.

## Results and Discussion

The formulation described in this paper was applied to both one-dimensional nozzle flows and axisymmetric flows over spherical blunt bodies.

The nozzle flows were treated using the governing equations for quasi-one-dimensional flow. Following Wilson and MacCormack [4], one-dimensional test cases were used to determine the suitability of CUSP for reactive flow simulations. Jachimowski's model of 9 species and 19 reactions for hydrogen/air was chosen. The nozzle is depicted in Figure 1 and had 256 cells in the streamwise direction. A supersonic inlet was used to achieve supersonic flow at the throat, while a back pressure was imposed to cause a shock to stand in the diverging section of the nozzle. The case presented here had an inlet Mach number of 6.1, temperature of 265 K and pressure of 23500 Pa. The inlet flow was stoichiometric hydrogen/air. The back pressure was set at 1.67 MPa, which caused a shock with upstream Mach number of 5.42 to form. The large increase in temperature (Figure 2) across the shock leads to radical production. When sufficient amounts of radicals have been created, water vapor is formed, heat is released and the temperature of the flow increases. In addition, a comparison of the density, temperature and pressure jumps across the shock with those from the normal shock relations reveals a high degree of accuracy in the flow solver. The results are quite satisfactory and agree closely with the results of Wilson and MacCormack.

The first axisymmetric case considered was a non-reacting flow over a  $25^\circ$  cone at a free stream Mach number of 5. This case was intended to test the accuracy of the axisymmetric formulation, since an exact solution exists for supersonic flow over a cone. Figure 3 shows the numerical solution computed on a  $64 \times 64$  grid; the variable shown is pressure normalized by the free stream pressure. The exact shock angle is  $30.5^\circ$  while the computed solution has a shock angle of  $30.4^\circ$ . Note that, as is found in the exact solution, the numerical solution exhibits constant properties on rays extending from the tip of the cone.

Stoichiometric hydrogen/oxygen flow over an axisymmetric spherical tip projectile at  $M = 3.55$  was computed using the reduced chemistry model (six species, eight reactions) of Evans and Schexnayder [1]. This corresponds to an experiment conducted by Lehr [21] which is shown in Figure 4. The diameter of this projectile is 15 mm. The free stream

temperature is 292 K and the free stream pressure is 24800 Pa. The grid in this case was  $64 \times 64$  cells. As shown in Figure 5, the bow shock in front of the body raises the temperature of the flow so that, after an induction zone, the flow reacts. The length of the induction zone varies depending on the post shock temperature which corresponds to the relative strength of the shock. Figure 6 shows that temperature is approximately constant in the induction zone as radicals build up to the necessary levels to react and produce water vapor. The production of water vapor is accompanied by heat release which raises the temperature and, because pressure is nearly constant across the reaction zone, lowers the density. The growth and destruction of radical species is depicted in Figure 7. Exponential growth can be observed in the induction zone, which is to be expected. By comparing Figure 4 and Figure 5, it is seen that the agreement between the computation and experiment is quite good. This computation also agrees favorably with that of Yuengster et al. [8] who limited the cell Damköhler number such that heat release was spread out among two to three cells. No such limitation is necessary using the current formulation.

The parallel speedup for this case is shown in Figure 8. The large number of calculations per grid point (as compared to non-reacting flows) as well as the explicit algorithm leads to the high parallel efficiency achieved, even for this relatively small mesh.

The final axisymmetric case considered was a case computed by Matsuo et al. [5]. This is a stoichiometric hydrogen/air flow at  $M = 4.79$  over a spherical projectile with a diameter of 2.5 mm. Jachimowski's mechanism including 9 species and 19 reactions was used for this case. This case was computed on a  $128 \times 256$  grid. The free stream temperature for this case is the same as the previous case while the pressure is 42600 Pa. Figure 10 shows contours of temperature for the steady state result while Figures 11 and 12 show the density and pressure contours in the flow field. The induction zone for this case is much smaller than the previous case since the higher Mach number produces a larger temperature rise across the shock. This larger initial temperature in the induction zone produces radicals at a much higher rate which leads to a faster reaction. Again, the heat release and temperature increase is accompanied by a density drop. The CUSP scheme is seen to accurately capture the shock and reaction front without oscillation and unnecessary dissipation. These results agree quite well with Matsuo et al.

## Conclusions

An accurate solver for the steady-state Euler equations with chemical reactions has been developed, and preliminary results have been presented. These results indicate a high degree of parallel scalability due to the explicit nature of the spatial discretization and the use of a point implicit formulation for the chemical source terms. Use of the CUSP dissipation scheme yields accurate capture of shocks, reaction zones and reaction fronts for both one-dimensional and axisymmetric test cases.

## Acknowledgements

This work was funded by AFOSR-URI F49620-93-1-0427. The first author was supported in part by a Fannie and John Hertz Foundation/Princeton Research Center Fellowship.

## References

- [1] Evans, J. S. and Schexnayder, C. J., "Influence of Chemical Kinetics and Unmixedness on Burning in Supersonic Hydrogen Flames", *AIAA Journal*, Vol. 18, No. 2, pp. 180-193, February 1980.
- [2] Jachimowski, C. J., "An Analytical Study of the Hydrogen-Air Reactions Mechanism With Application to Scramjet Combustion", NASA TP-2791, 1988.
- [3] Gardiner, W. C., Jr., *Combustion Chemistry*, Springer-Verlag, New York, 1984.
- [4] Wilson, G. J. and MacCormack, R. W., "Modeling Supersonic Combustion Using a Fully Implicit Numerical Method", *AIAA Journal*, Vol. 30, No. 4, pp. 1008-1015, April 1992.
- [5] Matsuo, A., Fujii, K. and Fujiwara, T., "Flow Features of Shock-Induced Combustion Around Projectile Traveling at Hypervelocities", *AIAA Journal*, Vol. 33, No. 6, pp. 1056-1063, June 1995.
- [6] Matsuo, A. and Fujiwara, T., "Numerical Investigation of Oscillatory Instability in Shock-Induced Combustion Around a Blunt Body", *AIAA Journal*, Vol. 31, No. 10, pp. 1835-1841, October 1993.
- [7] Shuen, J. S. and Yoon, S., "Numerical Study of Chemically Reacting Flows Using a Lower-Upper Symmetric Successive Overrelaxation Scheme", *AIAA Journal*, Vol. 27, No. 12, pp. 1752-1760, December 1989.

- [8] Yungster, S., Eberhardt, S. and Bruckner, A. P., "Numerical Simulation of Hypervelocity Projectiles in Detonable Gases", *AIAA Journal*, Vol. 29, No. 2, pp. 187-199, February 1991.
- [9] Bussing, T. R. A. and Murman, E. M., "Finite-Volume Method for the Calculation of Compressible Chemically Reacting Flows", *AIAA Journal*, Vol. 26, No. 9, pp. 1070-1078, September 1988.
- [10] Wilson, G. J. and Sussman, M. A., "Computation of Unsteady Shock-Induced Combustion Using Logarithmic Species Conservation Equations", *AIAA Journal*, Vol. 31, No. 2, pp. 294-301, February 1993.
- [11] Sussman, M. A., "Source Term Evaluation for Combustion Modeling", *AIAA Paper 93-0239*, *AIAA 31st Aerospace Sciences Meeting and Exhibit*, Reno, NV, January 11-14, 1993.
- [12] Eklund, D. R., Drummond, J. P. and Hassan, H. A., "Efficient Calculation of Chemically Reacting Flow", *AIAA Journal*, Vol. 25, No. 6, pp. 855-856, June 1987.
- [13] Martinelli, L., "Calculation of Viscous Flows with a Multigrid Method", Ph.D. Dissertation, Mechanical & Aerospace Engineering Department, Princeton University, October, 1987.
- [14] Gear, C. W., "Numerical Initial Value Problems in Ordinary Differential Equations", Prentice Hall, Englewood Cliffs, New Jersey, 1971.
- [15] Yee, H. C. and Shinn, J. L., "Semi-Implicit and Fully Implicit Shock-Capturing Methods for Nonequilibrium Flows", *AIAA Journal*, Vol. 27, No. 3, pp. 299-307, March 1989.
- [16] Bussing, T. R. A. and Murman, E. M., "Numerical Investigation of Two-Dimensional H<sub>2</sub>-Air Flameholding over Ramps and Rearward-Facing Steps", *Journal of Propulsion*, Vol. 3, No. 5, pp. 448-454, September-October 1987.
- [17] Eklund, D. R., Drummond, J. P. and Hassan, H. A., "Calculation of Supersonic Turbulent Reacting Coaxial Jets", *AIAA Journal*, Vol. 28, No. 9, pp. 1633-1641, September 1990.
- [18] Yungster, S. and Bruckner, A. P., "Computational Studies of a Superdetonative Ram Accelerator Mode", *Journal of Propulsion and Power*, Vol. 8, No. 2, pp. 457-463, March-April 1992.
- [19] Ju, Y., "Lower-Upper Scheme for Chemically Reacting Flow with Finite Rate Chemistry", *AIAA Journal*, Vol. 33, No. 8, pp. 1418-1425, August 1995.
- [20] Eberhardt, S. and Imlay, S., "Diagonal Implicit Scheme for Computing Flows with Finite Rate Chemistry", *Journal of Thermophysics and Heat Transfer*, Vol. 6, pp. 208-215, 1992.
- [21] Lehr, H. F., "Experiments on Shock-Induced Combustion", *Astronautica Acta*, Vol. 17, pp. 589-596, 1972.
- [22] Jameson, A., "Analysis and Design of Numerical Schemes for Gas Dynamics 1, Artificial Diffusion, Upwind Biasing, Limiters and their Effect on Multigrid Convergence", *International Journal of Computational Fluid Dynamics*, Vol. 4, pp. 171-218, 1995.
- [23] Jameson, A., "Analysis and Design of Numerical Schemes for Gas Dynamics 2, Artificial Diffusion and Discrete Shock Structure", *International Journal of Computational Fluid Dynamics*, Vol. 5, pp. 1-38, 1995.
- [24] Denton, J. D., "An Improved Time Marching Method for Turbomachinery Flow Calculations", *Journal of Engineering for Gas Turbines and Power*, Vol. 105, 1983.
- [25] Tatsumi, S., Martinelli, L., and Jameson, A., "Design, Implementation, and Validation of Flux Limited Schemes for the Solution of the Compressible Navier-Stokes Equations", *AIAA Paper 94-0647*, *AIAA 32nd Aerospace Sciences Meeting*, Reno, NV, January 1994.
- [26] Martinelli, L. and Jameson, A., "Validation of a Multigrid Method for the Reynolds Averaged Equations," *AIAA Paper 88-0414*, *AIAA 26th Aerospace Sciences Meeting*, Reno, NV, January, 1988.
- [27] Jameson, A., "Artificial Diffusion, Upwind Biasing, Limiters, and their Effect on Accuracy and Multigrid Convergence in Transonic and Hypersonic Flow," presented at the *AIAA 11th Computational Fluid Dynamics Conference*, Orlando, July 1993.
- [28] Oran, E. S. and Boris, J. P., *Numerical Simulation of Reactive Flow*, Elsevier, New York, 1987.



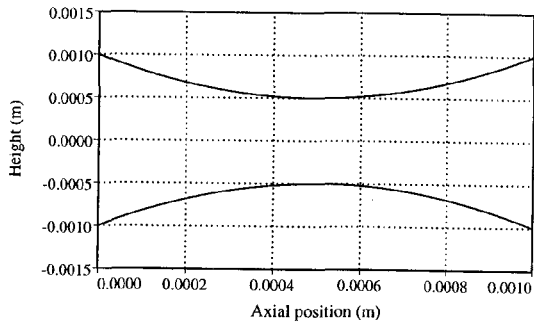


Figure 1: Nozzle geometry.

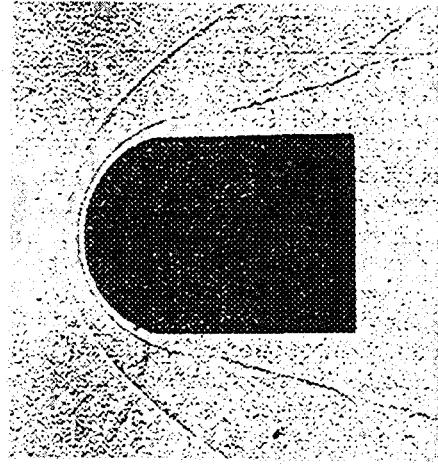


Figure 4: Experimental shockwave and reaction front— $M = 3.55$  hydrogen/oxygen, from Lehr [21].

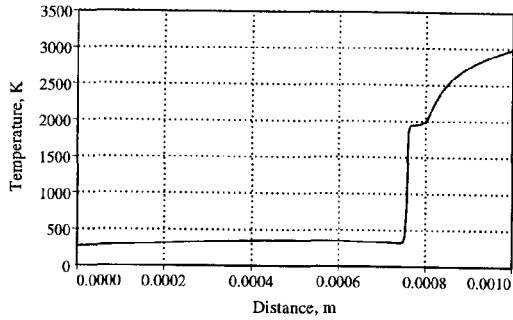


Figure 2: Temperature in the 1-D nozzle.

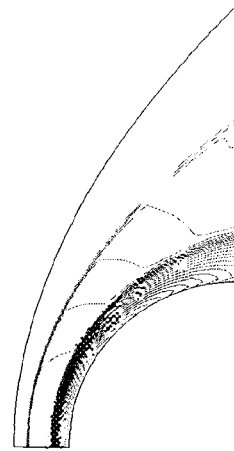


Figure 5: Temperature contours— $M = 3.55$  hydrogen/oxygen.

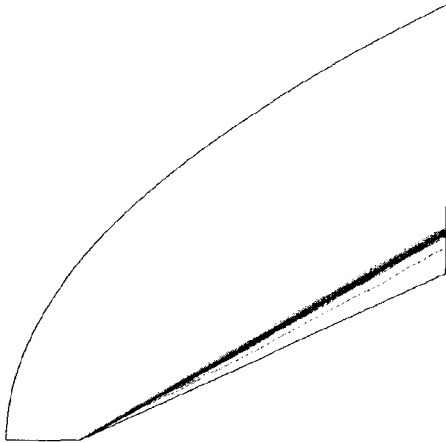


Figure 3: Normalized pressure over a 25° cone.

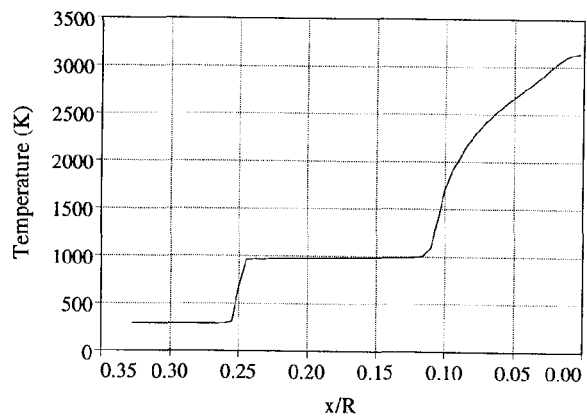


Figure 6: Temperature along stagnation streamline— $M = 3.55$  hydrogen/oxygen.

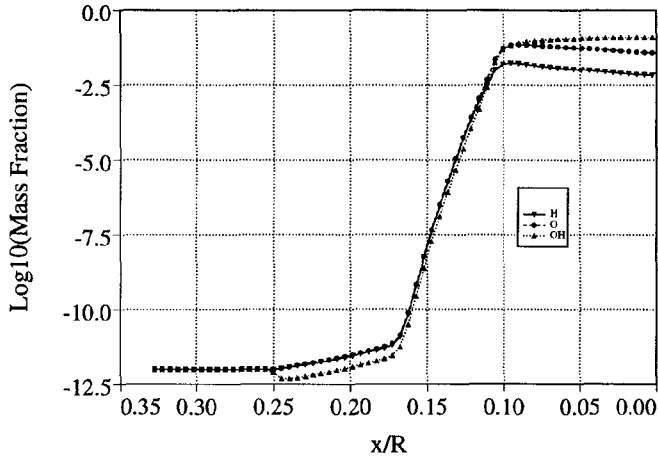


Figure 7: Logarithm of radical mass fractions along stagnation streamline— $M = 3.55$  hydrogen/oxygen.

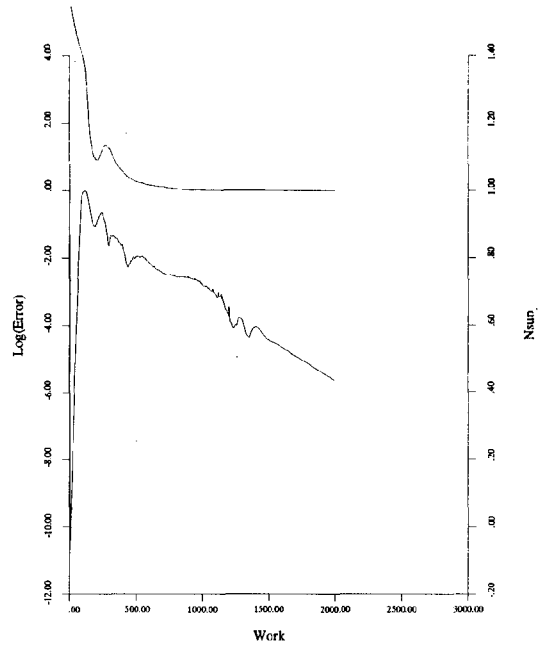


Figure 9: Convergence history— $M = 3.55$  hydrogen/oxygen.

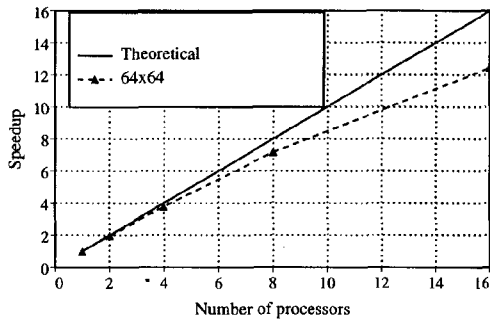


Figure 8: Parallel speedup for  $M = 3.55$  case.



Figure 10: Temperature contours— $M = 4.79$  hydrogen/air.

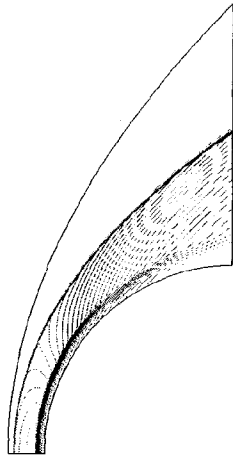


Figure 11: Density contours- $M = 4.79$  hydrogen/air.

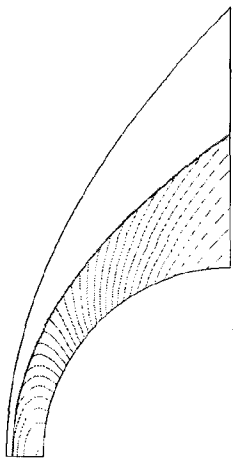


Figure 12: Pressure contours- $M = 4.79$  hydrogen/air.